Tip Characterization from AFM Images of Nanometric Spherical Particles

Kathryn A. Ramirez-Aguilar and Kathy L. Rowlen*

Department of Chemistry and Biochemistry, University of Colorado, Boulder, Colorado 80309

Received November 20, 1997. In Final Form: February 18, 1998

Since atomic force microscopy (AFM) images are a composite of probe and sample geometry, accurate size determinations are problematic. A relatively straightforward mathematical procedure for determining tip radius of curvature (R_T) for an asymmetrical tip was recently developed by Garcia et al. (*Probe Microsc.* **1997**, *1*, 107). This study represents an experimental test of that procedure for both silica (∼150 nm) and polystyrene (∼50 nm) nanospheres. The procedure can be summarized by two steps: (1) tip characterization assuming that the observed AFM height is a true measure of a spherical particle's diameter and (2) use of the tip shape to extract a calculated width. To ensure that AFM heights were equivalent to the true width, a direct comparison of individual particle sizes determined by transmission electron microscopy (TEM) and AFM was conducted. Heights measured from AFM images of polystyrene nanospheres differed, on average, less than 5% from widths measured by TEM. The quality of R_T values was therefore evaluated by the magnitude of relative error in calculated particle widths with respect to true widths. For the tip used in this study a calculated R_T of 13 nm resulted in excellent calculated widths for both polystyrene and silica spheres. While spherical particles whose diameter is less than R_T (such as 5-nm Au colloids) can be used to characterize the tip apex, larger diameter spheres are required to fully characterize the tip. However, spheres much larger than R_T predominantly interact with the walls of the tip and therefore yield artificially high R_T values. On the basis of our analysis of the procedure developed by Garcia et al., the best sphere size for full characterization of the tip (apex and walls) is one in which both portions of the tip interact with the sphere to similar extents (approximately: $R_T \leq R_p \leq 2R_T$, where R_p is the particle radius).

Introduction

AFM is a powerful technique for studying the micro- and nanoscopic world because the measurement of three-dimensional surface topography is straightforward and can be applied under a wide variety of sample conditions.[2,3] As a result, AFM has found applications in fields ranging from semiconductor physics[4−7] to biology.[8−10] In addition, several variations on the imaging "mode" have been developed, enabling investigation of physical properties such as friction,[11,12] magnetism,[13,14] surface charge,[15,16] rigidity,[17,18] and capacitance.[19,20]

One of the difficulties associated with quantitative analysis of AFM images stems from the fact that AFM requires probe−sample contact, resulting in a composite image of both the probe (tip) and the sample geometry. Therefore AFM images of a particular sample vary depending upon tip shape.[21] When both the sample geometry and the geometry of the imaging portion of the tip are unknown, an AFM image contains little quantitative information. Justifiably, a great deal of effort has gone into the development of algorithms for extracting true tip and surface feature metrics. Several researchers have proposed algorithms for removing the geometric effects of a symmetrical tip apex from AFM images.[22−26] Attempts to extract true tip shape, including the walls of the tip beyond the apex, have been reasonably successful for images of surface features of known shape and size.[3,22,23,26,27] Only a few "reconstruction" approaches treat the asymmetry often observed in the probe tips.[28,29] A mathematical procedure recently reported by Garcia et

* To whom correspondence should be addressed.

(1) Garcia, V. J.; Martinez, L.; Briceno-Valero, J. M.; Schilling, C. H. *Probe Microsc.* **1997**, *1*, 107.
(2) Howland, R.; Benatar, L. *A Practical Guide to Scanning Probe Microscopy*, Park Scientific Instruments: Sunnyvale, CA, 1993; Chapters 1 and 2.
(3) Griffith, J. E.; Grigg, D. A. *J. Appl. Phys.* **1993**, *74*, R83.
(4) Smith, I.; Howland, R. *Solid State Technol.* **1990**, *33* (12), 53.
(5) Yoon, J.; Ivey, D. G. *J. Mater. Sci. Lett.* **1996**, *15*, 551.
(6) Krausch, G.; Colchero, J.; Detzel, T.; Fink, R.; Luckscheiter, B.; Wohrmann, U.; Schatz, G. *Hyperfine Interact.* **1993**, *78*, 295.
(7) Abe, T.; Steigmeier, E. F.; Hagleitner, W.; Pidduck, A. J. *Jpn. J. Appl. Phys.* **1992**, *31*, 721.
(8) Shao, Z.; Mou, J.; Czajkowsky, D. M.; Yang, J.; Yuan, J.-Y. *Adv. Phys.* **1996**, *45*, 1.
(9) Kasas, S.; Thomson, N. H.; Smith, B. L.; Hansma, P. K.; Miklossy, J.; Hansma, H. G. *Int. J. Imaging Syst. Tecnol.* **1997**, *8*, 151.
(10) Haggerty, L.; Lenhoff, A. M. *Biotechnol. Prog.* **1993**, *9*, 1.
(11) Fujihira, M.; Morita, Y. *J. Vac. Sci. Technol., B* **1994**, *12*, 1609.
(12) Frisbie, C. D.; Rozsnyai, L. F.; Noy, A.; Wrighton, M. S.; Lieber, C. M. *Science* **1994**, *265*, 2071.
(13) Martin, Y.; Wickramasinghe, H. K. *Appl. Phys. Lett.* **1987**, *50*, 1455.
(14) DiCarlo, A.; Scheinfein, M. R.; Chamberlin, R. V. *Appl. Phys. Lett.* **1992**, *61*, 2108.
(15) Yoo, M. J.; Fulton, T. A.; Hess, H. F.; Willett, R. L.; Dunkleberger, L. N.; Chichester, R. J.; Pfeiffer, L. N.; West, K. W. *Science* **1997**, *276*, 579.
(16) Sugawara, Y.; Fukano, Y.; Uchihashi, T.; Okusako, T.; Morita, S.; Yamanishi, Y.; Oasa, T.; Okada, T. *J. Vac. Sci. Technol., B* **1994**, *12*, 1627.
(17) Maivald, P.; Butt, H. J.; Gould, S. A. C.; Prater, C. B.; Drake, B.; Gurley, J. A.; Elings, V. B.; Hansma, P. K. *Nanotechnology* **1991**, *2*, 103.
(18) Persch, G.; Born, C.; Engelmann, H.; Koehler, K.; Utesch, B. *Scanning* **1993**, *15*, 283.
(19) Neubauer, G.; Erickson, A.; Williams, C. C.; Kopanski, J. J.; Rodgers, M.; Adderton, D. *J. Vac. Sci. Technol., B* **1996**, *14*, 426.
(20) Erickson, A.; Sadwick, L.; Neubauer, G.; Kopanski, J.; Adderton, D.; Rodgers, M. *J. Electron Mater.* **1996**, *25*, 301.
(21) Howald, L.; Haefke, H.; Lüthi, R.; Meyer, E.; Gerth, G.; Rudin, H.; Güntherodt, H.-J. *Phys. Rev. B* **1994**, *49*, 5651.
(22) Markiewicz, P.; Goh, M. C. *Langmuir* **1994**, *10*, 5.
(23) Markiewicz , P.; Goh, M. C. *J. Vac. Sci. Technol., B* **1995**, *13*, 1115.
(24) Nagase, M.; Namatsu, H.; Kurihara, K.; Makino, T. *Jpn. J. Appl. Phys.* **1996**, *35*, 4166.
(25) Keller, D. *Surf. Sci.* **1991**, *253*, 353.
(26) Keller, D. J.; Franke, F. S. *Surf. Sci.* **1993**, *294*, 409.
(27) Markiewicz, P.; Goh, M. C. *Rev. Sci. Instrum.* **1995**, *66*, 3186.
(28) Vesenka, J.; Miller, R.; Henderson, E. *Rev. Sci. Instrum.* **1994**, *65*, 2249.

S0743-7463(97)01277-8 CCC: $15.00 © 1998 American Chemical Society
Published on Web 04/09/1998

Table 1. Comparison of AFM and TEM Size Values for Polystyrene Nanospheres[a]

sphere	TEM width nm)	AFM height (nm)	relative error (in the height) (%)	AFM width (nm)	relative error (in the width) (%)
1	30.5 ± 0.5	29.1 ± 0.2	4.6	65.3 ± 0.5	114
2	44.1 ± 0.5	45.7 ± 0.3	3.6	87.6 ± 0.3	99
3	35.0 ± 0.5	37.0 ± 0.2	5.7	76.2 ± 0.4	118
4	44.1 ± 0.5	45.7 ± 0.5	3.6	89.6 ± 0.4	103
5	36.8 ± 0.5	38.5 ± 0.9	4.6	77 ± 2	109

[a] TEM widths were measured directly from the negatives using a calibrated magnification monocular. The reported TEM values are the average of two measurements, and the error is the average difference in the two values. AFM heights were obtained from bearing analysis software (Digital Instrument v 4.23r2) with the box cursor. AFM widths were determined from the bearing analysis software with the line cursor. For AFM, the mean ±1s from three measurements is reported. Relative error is defined with respect to the measured TEM widths.

al.[1] for extracting true widths from images of spherical particles takes into account both the tip apex and walls as well as possible asymmetry in the tip shape. Perhaps the most important advantage of the "Garcia procedure" is that each of the necessary variables required for the extraction of true widths from images of spherical particles can be obtained directly from the AFM images in a straightforward analysis of particle width/height pairs.

In the study reported here, the procedure developed by Garcia et al.[1] was experimentally tested. Both relatively large nanospheres (silica, ∼150 nm) and mid-sized nanospheres (polystyrene, ∼50 nm) were used to characterize the radius of curvature (R_T) for a single tip. The quality of each R_T value was evaluated by the magnitude of relative error in widths calculated using R_T.

Experimental Procedure

Sample Preparation. A 2.9 × 10^{14} particle/mL aqueous suspension of ∼50-nm-diameter polystyrene spheres in 10% surfactant was purchased from Duke Scientific. A 3.036 × 10^{13} particle/mL aqueous suspension of ∼150-nm-diameter 3-aminopropyl silica spheres was purchased from Bangs Laboratory. A 1-μL aliquot of the polystyrene stock was diluted into 0.5 mL of methanol (Burdick and Jackson, HPLC grade) in an Optimum polypropylene 0.65-mL microcentrifuge tube. A 2-μL aliquot of the silica stock was diluted to 0.25 mL in the same manner. The diluted polystyrene suspension was sonicated for 45 s. The diluted silica suspension was sonicated for 10 min. Immediately after sonication, 5 μL of each suspension was deposited onto a carbon-coated Formvar film on a 200 mesh-copper Index II TEM locator grid (Ted Pella Cat # 79022C).

Imaging. Polystyrene and silica samples were imaged by AFM in air at room temperature using a Digital Instruments Nanoscope IIIa Multimode. All images were obtained using tapping mode imaging with a single TESP silicon probe (Force constant of 20−100 N/m, Digital Instruments). The scan angle was maintained at 0°, and the images were captured in the trace direction with a scan rate of 0.5 Hz. To locate individual polystyrene nanospheres for imaging by both TEM and AFM, a top-view optical microscope was used to establish a position on the TEM grid,[30] which could be viewed through the carbon-Formvar film, while imaging by AFM. TEM images of silica and polystyrene samples were obtained using a JEOL 100C transmission electron microscope with an accelerating voltage of 80 kV.

Sphere Measurements. Height and width measurements from AFM images were made with Digital Instruments Nanoscope Software version 4.23r2. Prior to making measurements, the "zoom and planefit" function was applied to each sphere in the images. AFM height measurements in Table 1 were made by using the box cursor in bearing analysis. All other height and width measurements were obtained using the bearing analysis line cursor. In cases where the line cursor was used, cross-sections were always drawn with a perfectly horizontal line (with respect to the scan direction) in order to evaluate data from a single scan line. Since section analysis is typically used to evaluate height and width in AFM images, a quantitative study was undertaken to test agreement in measurements made using bearing analysis versus those made using section analysis. For a relatively large data set (>150 measurements using 5 polystyrene spheres), regardless of how sphere images were modified (zooming, zooming and planefitting, zooming and flattening), height and width measurements between the two methods differed, on average, by less than 3%.

Results and Discussion

Figure 1 is a direct comparison of five individual polystyrene nanospheres imaged by both AFM (a) and TEM (b). Both images have a 600 nm × 600 nm $x-y$ scale. Clearly, the widths are broadened significantly by tip geometric effects in the AFM image. The measured size values for the spheres shown in Figure 1 are summarized in Table 1. Although polystyrene is somewhat compressible, Li and Lindsay[31] have shown that polystyrene nanospheres show negligible deformation with contact forces as high as 15 nN. As anticipated for the low-force imaging achieved by tapping mode, the height values determined for polystyrene by AFM are within ∼5% relative error of the widths determined by TEM. AFM measurements are known to be affected by relative humidity;[32,33] however, the agreement between the TEM widths and the AFM heights is indicative of a negligible influence from the adsorbed water layer (present at relative humidities greater than 10%). Other studies have performed statistical comparisons of TEM and AFM values (not direct comparison of individual particles) for nanometric gold particles[34,35] and have reported similar results. Figure 2 is a representative TEM image of the silica particles used in this study. While it is clear that not all of the particles are spherical,[36,37] an effort was made to utilize only spherical particles for quantitative analysis. Specifically, top-view AFM images of each silica particle were evaluated for symmetry prior to use in height/width measurements.

Figure 3 is a measured cross-section of the fourth sphere from the top of the AFM image in Figure 1a. The probe used to obtain the tapping mode image was an asymmetrical, pyramidal-shaped silicon tip. These tips are reported to have front and back half angles of 10° and 25°,

(29) Wilson, D. L.; Kump, K. S.; Eppell, S. J.; Marchant, R. E. *Langmuir* **1995**, *11*, 265.
(30) Markiewicz, P.; Goh, M. C. *Ultramicroscopy* **1997**, *68*, 215.
(31) Li, Y.; Lindsay, S. M. *Rev. Sci. Instrum.* **1991**, *62*, 2630.
(32) Thundat, T.; Warmack, R. J.; Allison, D. P.; Bottomley, L. A.; Lourenco, A. J.; Ferrell, T. L. *J. Vac. Sci. Technol., A* **1992**, *10*, 630.
(33) Vesenka, J.; Manne, S.; Yang, G.; Bustamante, C. J.; Henderson, E. *Scanning Microsc.* **1993**, *7*, 781.
(34) Vesenka, J.; Manne, S.; Giberson, R.; Marsh, T.; Henderson, E. *Biophys. J.* **1993**, *65*, 992.
(35) Graber, K. C.; Brown, K. R.; Keating, C. D.; Stranick, S. J.; Tang, S.-L.; Natan, M. J. *Anal. Chem.* **1997**, *69*, 471.
(36) Stober, W.; Fink, A. *J. Colloid Interface Sci.* **1968**, *26*, 62.
(37) van Blaaderen, A.; Kentgens, A. P. M. *J. Noncryst. Solids* **1992**, *149*, 161.

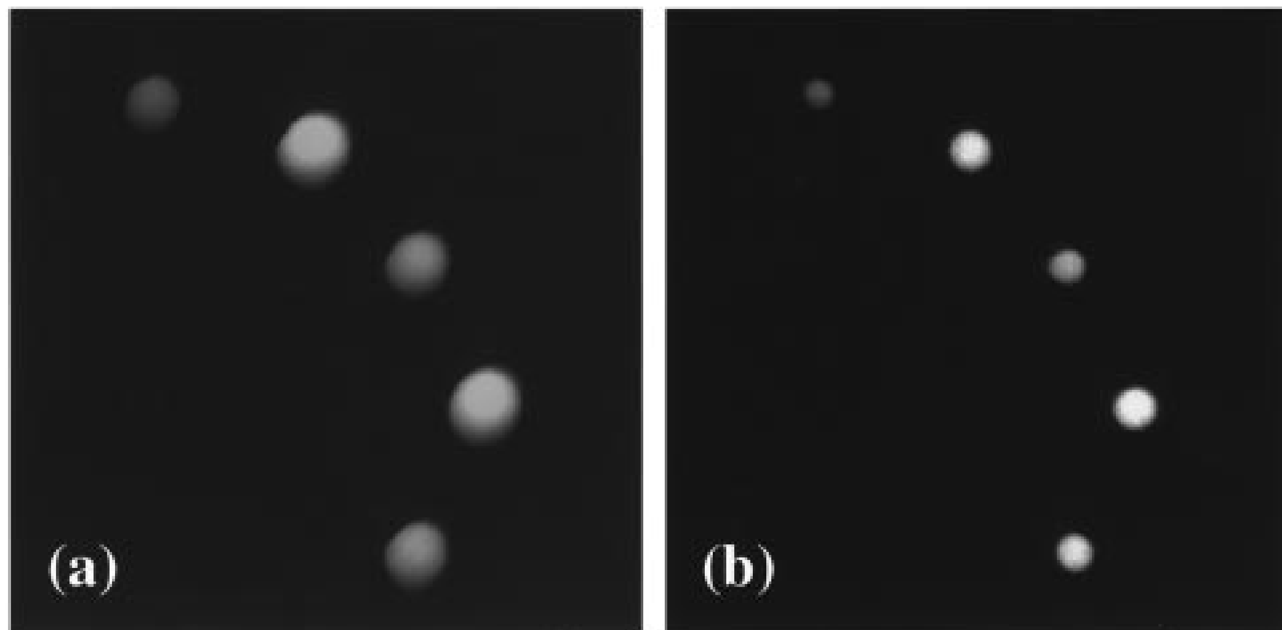

Figure 1. (a) Tapping mode AFM image and (b) TEM image of polystyrene nanospheres deposited onto a carbon-Formvar-coated TEM grid. Both images are 600 nm × 600 nm. In the AFM image, increasing values along the *z*-axis are represented as lighter shades of gray. The magnification of the TEM image is 110 000. As referred to in the text, the spheres are numbered in increasing order from top to bottom.

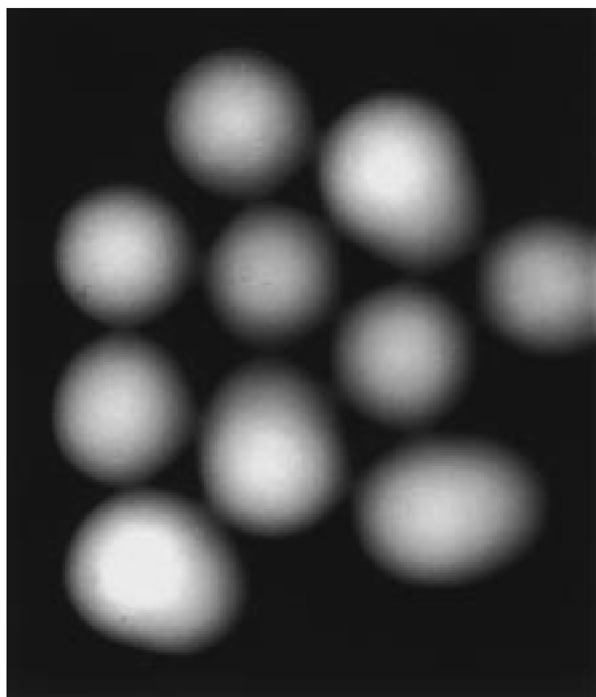

Figure 2. TEM (magnification 110 000) of silica "nanospheres" deposited onto a carbon-Formvar-coated copper grid. The image size is 600 nm × 700 nm. Although the nanospheres are grouped in this image, only individual nanospheres were used in the study.

respectively.[38,39] Assuming that the tip-cantilever base is positioned perfectly in the holder and a 0° scan angle is used with trace capture, surface features first encounter the 10° tip slope. A representative tip shape is shown superimposed on the cross-sectional view of a sphere drawn to-scale in Figure 3. The cross-section of the sphere's AFM image can be visualized by mapping the tip across the surface of the sphere using the first point-of-contact to mark tip position. The tip's position at point-of-contact is recorded, roughly, at the position of the tip apex.[29] Other imaging factors, such as piezoelectric scanner hysteresis and drift, can contribute to asymmetry in the cross-section.[2,40]

The Model. The model tested in this study for calculation of R_T and extraction of true widths is given in detail in ref 1; therefore, only a brief outline is given here. The procedure can be summarized by two steps: (1) tip characterization assuming that the height is a true measure of a spherical particle's diameter and (2) use of the tip shape to extract a calculated width. The validity of the assumption in step 1 was verified by the results reported in Table 1. Since spherical particles were imaged, the widths calculated in step 2 were used to evaluate the quality of the tip characterization step.

To fully characterize the tip, it is necessary that both the apex and walls of the tip interact to a significant extent with the particle to be imaged. The model developed by Garcia et al.[1] allows for the use of spherical particles partially embedded in the substrate, as might be the case for particles deposited onto a "soft" surface. However, on the basis of the direct comparison of AFM heights with TEM widths, summarized in Table 1, it was demonstrated that the particles used in this study are not embedded in the polymer substrate. Therefore, the minimum particle radius, R_p, required to fully characterize the tip can be calculated from[1]

$$R_p \geq R_T \frac{(K-1)}{(K+1)} \tag{1}$$

where $K = K_{max} = [1 + (\tan(90 - \beta))^2]^{1/2}$ and β is the tip slope (i.e., the half angle of a given tip edge). As shown in Figure 3, the TESP tips sold by Digital Instruments for tapping mode imaging have two nonequivalent slopes for

(38) *Specification Table for Deflection Mode Cantilevers*; Digital Instruments, Inc.: Santa Barbara, CA (1-17-95).
(39) Multimode SPM Instruction Manual, Ver. 4.31ce; Digital Instruments, Inc.: Santa Barbara, CA, 1996–97; Chapter 4.
(40) *Artifacts in SPM*; TopoMetrix Corporation: Santa Clara, CA, 1993; Chapter 3.

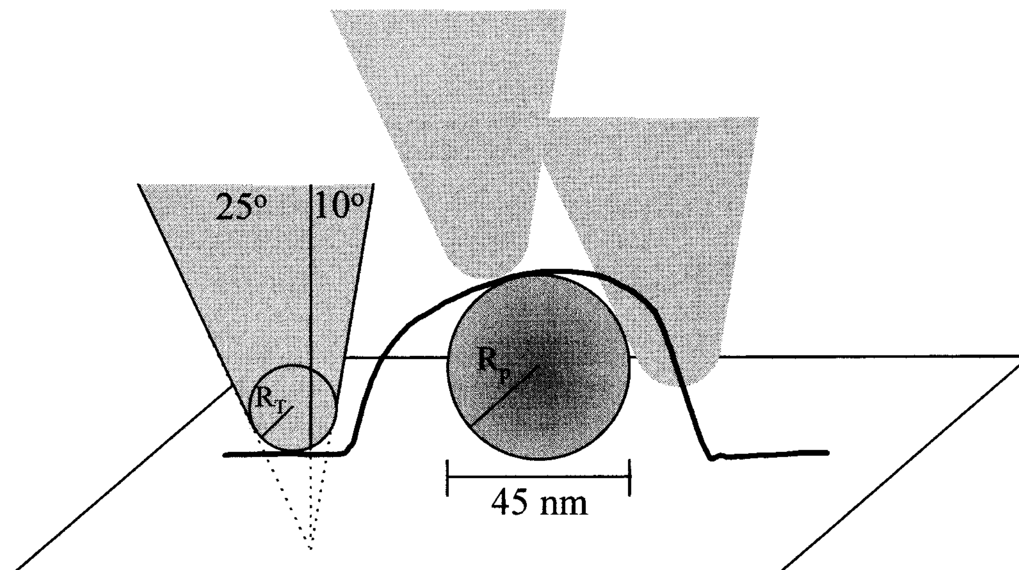

Figure 3. Measured cross-section of sphere number 4 in Figure 1a. For viewing purposes a true sphere and a model tip are drawn to scale. The apex of the tip is a sphere with a radius of curvature R_T. The half-cone angles are drawn with respect to a virtual tip apex (shown below the image plane in the figure).

a 0° scan angle. Typical R_T values for these tips, as specified by the manufacturer, are 5−10 nm.[38] For an R_T of 10 nm and a β value of 25° the minimum particle radius is 4 nm. For an R_T of 10 nm and a β value of 10°, the minimum particle radius is 7 nm. Thus, both the silica (~75 nm radius) and the polystyrene (~25 nm radius) spheres used in this study should be suitable for full tip characterization.

For a spherical surface feature which interacts with both the tip apex and walls, the resulting composite image can be described by the following equation:

$$W = C_1(h - R_p) + C_2R_p + C_3R_T \quad (2)$$

where W is the image width, h is the vertical distance between the top of the sphere and a lower point on the sphere, R_p is the true radius of the sphere, and R_T is the radius of curvature for the tip apex. The coefficients C_1, C_2, and C_3 are related to the tip symmetry.[1] If W is measured where $h = R_p$, that is, at half the maximum height, a plot of W versus R_p for a number of spheres, with different radii, yields a line with a slope of C_2 and an intercept of C_3R_T. C_1 is obtained by plotting sets of W versus $h - R_p$ for a given sphere; that is, the width is measured at various heights for a given sphere. In this case, the slope of the linear region is C_1 and the intercept is irrelevant. C_3 is equal to $C_2 - C_1$. With these coefficients in hand, R_T may be calculated.

Once the tip has been characterized, the value for R_T can be used to calculate the true radius of the spherical feature using one of the following equations.

$$R_p = \frac{(W^2 + 4h^2)}{8h} - R_T \quad (3)$$

$$R_p = \frac{W - C_1h}{C_3} - R_T \quad (4)$$

Equation 3 is used at heights (h) on the particle at which only the tip apex is interacting with the particle, that is, near the top of a given sphere. Equation 4 is used at heights where there is significant interaction between the tip edge and the sphere. "Significant" interaction is defined with respect to a criterion established by Garcia et al.[1] Furthermore, the suitability of eq 3, which essentially models a sphere-on-sphere interaction, can be evaluated by determining whether the first term in the equation ($[W^2 + 4h^2]/8h$, which is referred to as the spherical form factor (SFF) by Garcia et al.) remains constant as a function of height. In this study, for polystyrene the SFF was deemed to be nonvariant if it changed less than 1 nm over a height range of at least 5 nm. For silica, the SFF was deemed to be nonvariant if it changed less than 1 nm over a height range of at least 15 nm. Height/width pairs that failed the SFF test were discarded.

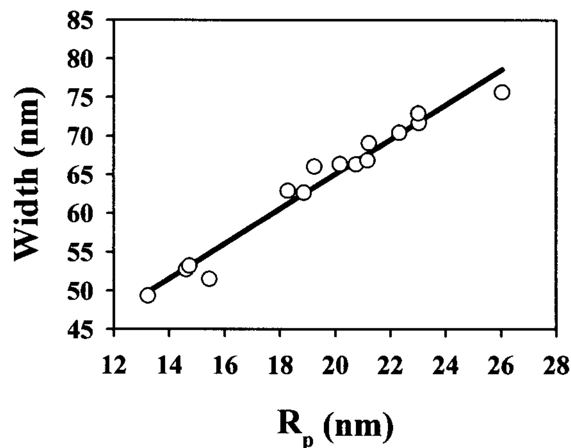

Figure 4. Width determined at half the maximum height versus R_p for 15 polystyrene nanospheres imaged by tapping mode AFM. As shown in Table 1, the height values determined by AFM and the width values determined by TEM are in excellent agreement. Therefore, R_p values were obtained by dividing the AFM height measurements by two. The equation for the linear regression (solid line) is $W = 2.2R_p + 20$.

Tip Characterization. Figure 4 is a graph of W versus R_p for 15 polystyrene nanospheres imaged by tapping mode AFM (including the 5 spheres shown in Figure 1). The slope of this graph yields C_2, and the intercept is C_3R_T ($=W_{intercept}$). For silica, this "C_2" graph was constructed using 5 spheres. Figure 5 is a *representative* graph of W versus $h - R_p$ for a silica sphere. Note that the slope in

Table 2. Evaluation of Tip Characterization (R_T) Based on Relative Error in Calculated Sphere Widths[a]

method	R_T	calculated sphere width (nm)					relative error (%)
		sphere 1	sphere 2	sphere 3	sphere 4	sphere 5	
case 1	22.6 ± 0.4	169 ± 3	148 ± 5	149 ± 4	152 ± 1	160 ± 1	3
case 2	12.9 ± 0.6	34 ± 3	51 ± 4	43 ± 4	52 ± 4	42 ± 4	13
case 3	12.9 ± 0.6	30.3 ± 0.3	47.2 ± 0.7	39.0 ± 0.3	48.2 ± 0.6	38.8 ± 0.4	4
case 4	22.6 ± 0.4	16.7 ± 0.8	36.1 ± 0.7	26.6 ± 0.7	37 ± 1	26.5 ± 0.7	28
case 5	12.9 ± 0.6	170 ± 10	151 ± 8	151 ± 7	147 ± 3	154 ± 2	3
case 6	12.9 ± 0.6	165 ± 3	150 ± 7	150 ± 6	147 ± 3	153 ± 3	2

[a] Presented in the table are calculated widths ($2R_p$) for the five polystyrene spheres shown in Figure 1a and five silica particles (AFM heights (nm): 165 ± 1; 152 ± 3; 145 ± 3; 154 ± 5; 150 ± 2). See text for an explanation of the six cases. Mean R_T values and the associated ±1s error are reported. Relative error was calculated as the difference between the width measured by AFM and the true width (as determined from height measurements in AFM) divided by the true width. The column titled relative error is the *average* relative error for the five spheres given in the table.

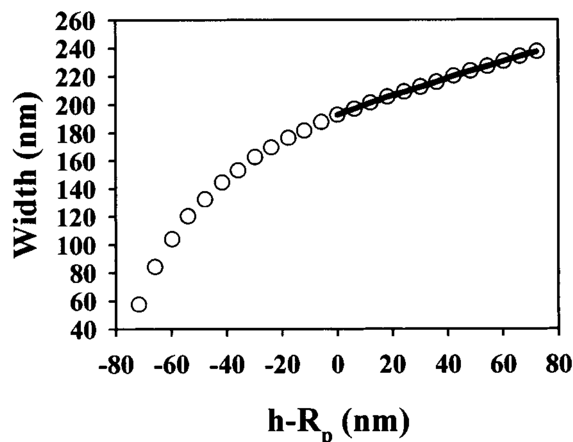

Figure 5. AFM measured widths versus $h - R_p$ (where h is height) shown for a silica sphere. The equation for the linear regression (solid line) is $W = 0.61(h - R_p) + 194$.

this case is not linear over the entire height of the sphere; C_1 is therefore determined from the slope of the linear region, which, of course, results in associated error. Average C_1 values were obtained by evaluating a minimum of 5 spheres for both silica and polystyrene. Using the values obtained from these two graphs, R_T is calculated from $W_{intercept}/(C_2 - C_1)$.

As summarized in Table 2, R_T values were calculated, and their accuracy was evaluated for several cases: (1) silica nanospheres, (2) polystyrene nanospheres, and (3) polystyrene nanospheres for which K_{min} (rather than K_{max}) was used in the determination of the appropriate equation. In addition, the R_T value calculated from silica particles was used to extract widths from AFM images of polystyrene spheres (case 4), and R_p values for silica particles were calculated from polystyrene-based R_T values (cases 5 and 6). K_{max} was used for case 5 and K_{min} was used in case 6.

For case 1, where the relatively large silica particles were used to characterize the tip, the calculated R_T is significantly outside the specified range of 5−10 nm.[38] Use of the silica-based R_T value does yield a low average relative error in the calculated width for silica spheres. In case 2, K_{max} was used in the determination of the appropriate equation (eq 3 or 4) to apply for calculation of R_p. Note that the calculated width for this case has a large average relative error (13%). Recall that K is related to the slope of the tip wall. Garcia et al. give three options for the choice of K, since, in reality, it is likely to be a complicated function rather than a linear slope.[1] For case 3, K was calculated using the 25° tip slope, in contrast to the use of the 10° tip slope for K_{max}. Note that case 3 yields a much lower average relative error in the calculated sphere width, only 4%.

To evaluate the "universality" of a given R_T, the R_T value obtained for silica spheres was used to extract widths from AFM images of polystyrene spheres. This case, 4, results in a very poor average relative error; that is, when large spheres are used to characterize the tip, attempts to extract true widths from smaller particles fail. This result is intuitive, since the larger silica spheres interact with the tip walls to a much greater extent than the polystyrene spheres (which are a factor of 3 smaller in diameter). However, when the R_T calculated from the analysis of polystyrene spheres is used to extract widths from AFM images of silica spheres, the average relative error is impressive (2−3%).

In summary, the calculated R_T value that results in the best calculated widths for both types of nanospheres is $R_T \sim 13$ nm. This value seems quite realistic considering that unused TESP tips, imaged by TEM, are reported to have R_T values <12 nm.[41] Overall, the procedure developed by Garcia et al.[1] is easy to use and appears to work well as a means to characterize AFM tips. On the basis of our analysis of the procedure developed by Garcia et al., the best sphere size for full characterization of the tip (apex and walls) is one in which both portions of the tip interact with the sphere to similar extents (approximately: $R_T \leq R_p \leq 2R_T$). While spherical particles with a diameter less than R_T (such as 5-nm Au colloids) can be used to characterize the tip apex, larger diameter spheres are required to fully characterize the tip. However, spheres much larger than R_T predominantly interact with the walls of the tip and therefore yield artificially high R_T values.

Acknowledgment. This work was supported by grants from the National Science Foundation (CHE-9634198 and EAR-9256339).

LA971277O

(41) DeRose, J. A.; Revel, J.-P. *Microsc. Microanal.* **1997**, *3*, 203.